Journal of Zhejiang University SCIENCE A
ISSN 1673-565X (Print); ISSN 1862-1775 (Online)
www.zju.edu.cn/jzus; www.springerlink.com
E-mail: jzus@zju.edu.cn

Environmental effects induced by excavation*

Yu-qi LI†[1,2], Jian ZHOU[2], Kang-he XIE[3]

([1]*Department of Civil Engineering, Shanghai University, Shanghai 200072, China*)

([2]*Department of Geotechnical Engineering, Tongji University, Shanghai 200092, China*)

([3]*Institute of Geotechnical Engineering, Zhejiang University, Hangzhou 310027, China*)

†E-mail: liyuqi2000@hotmail.com; liyuqi2000@shu.edu.cn

Received Aug. 21, 2006; revision accepted Nov. 27, 2006; published online Nov. 10, 2007

Abstract: Based on 3D Biot's consolidation theory and nonlinear Duncan-Chang's model, a 3D FEM (finite element method) program is developed considering the coupling of groundwater seepage and soil skeleton deformation during excavation. The comparison between the analysis result considering the variation of water head difference and that without considering it shows that the porewater pressure distribution of the former is distinctly different from that of the latter and that the foundation pit deformations of the former are larger than those of the latter, so that the result without considering the variation of water head difference is unreliable. The distribution rules of soil horizontal and vertical displacements around the pit and excess porewater pressure are analyzed in detail in time and space, which is very significant for guiding underground engineering construction and ensuring environment safety around the pit.

Key words: Environmental effect, Excavation, Deformation, Excess porewater pressure
doi:10.1631/jzus.A061434 **Document code:** A **CLC number:** TU433

INTRODUCTION

With the development of city construction, much underground space is utilized and many deep foundation pits sequentially appear. Excavation need not only ensure the stability and the safety of a pit, but also control the movement of soil stratum around and protect it from being damaged. Especially in some Chinese coastal areas, such as Shanghai, Guangzhou and Hangzhou, the soil strata are very soft and soil is often saturated, therefore excavation will result in large soil stratum movement. Movement induced by excavation greatly influences the safety of buildings, subways, underground pipelines and other municipal constructions around a pit, so the consequent environmental effects have become key problems in excavation and caused much attention. Hou and Chen (1989) investigated the rule of displacement in soil medium surrounding deep excavations and presented a method to evaluate the ground surface settlement. With the wide application of finite element technology, finite element analysis was used in many deep excavations and some basic rules of environmental effects of excavation were analyzed and investigated (Whittle *et al*., 1993; Ou and Lai, 1994; Zhang *et al*., 1999; Ping *et al*., 2001). The effect of ground settlement and lateral deflection induced by deep excavations on damage of buried pipelines was also discussed (Duan and Shen, 2005). Zdravkovic *et al*.(2005) studied the effect of excavation on the surrounding areas and provided a detailed assessment of wall and ground movements. In addition, Xie *et al*.(2002) theoretically confirmed that the changes in effective stresses resulted from dewatering during excavation and seepage were the main factors inducing settlement of ground surface by comparing the calculating results with the field measurements. Shi and Peng (2006) further presented a new method of calculating ground surface settlement caused by foundation pit excavation and dewatering based on

* Project supported by the China Postdoctoral Science Foundation (No. 20060400672) and Innovation Fund of Shanghai University, China

the stochastic medium theory, seepage theory and soil consolidation theory.

However, due to the complexity of excavation and groundwater seepage, study on environmental effects of excavation is not yet profound. By the effective stress analysis, not only groundwater seepage including seepage induced by unloading and seepage induced by the water head difference between the inside and outside of a pit, but also the coupling of groundwater seepage and soil skeleton deformation can be taken into account, so in this paper 3D consolidation finite element equations are derived, and the corresponding finite element program is further developed. Some useful conclusions are drawn by analyzing the influences of the water head difference between the inside and outside of a pit on excess porewater pressure and the pit deformations and then investigating the time and space variations of environmental effect.

FINITE ELEMENT EQUATIONS

Biot's 3D consolidation finite element equations (Xie and Zhou, 2002) are as follows:

$$[\boldsymbol{K}]\{\Delta \boldsymbol{U}\}^{\mathrm{e}} = \{\Delta \boldsymbol{R}\}^{\mathrm{e}}, \tag{1}$$

where $[\boldsymbol{K}]$ is the element consolidation matrix, $\{\Delta \boldsymbol{U}\}^{\mathrm{e}}$ is the increment column matrix of unknown terms of element node, and $\{\Delta \boldsymbol{R}\}^{\mathrm{e}}$ is the increment column matrix of equivalent load and water runoff of element node.

The submatrix of $[\boldsymbol{K}]$ can be expressed as:

$$[\boldsymbol{K}_{ij}] = \begin{bmatrix} [\boldsymbol{K}_{eij}] & [\boldsymbol{K}_{cij}] \\ [\boldsymbol{K}_{cji}] & -\theta \Delta t K_{sij} \end{bmatrix}, \tag{2}$$

where θ is the integral constant, Δt is the time increment, and the calculation of $[\boldsymbol{K}_{eij}]$, $[\boldsymbol{K}_{cij}]$ and K_{sij} can be found in (Xie and Zhou, 2002).

The submatrixes of $\{\Delta \boldsymbol{U}\}^{\mathrm{e}}$ and $\{\Delta \boldsymbol{R}\}^{\mathrm{e}}$ can be expressed as:

$$\{\Delta \boldsymbol{U}_i\} = [\Delta u_i \quad \Delta v_i \quad \Delta w_i \quad \Delta p_i]^{\mathrm{T}},\ i=1,2,\ldots,8, \tag{3}$$

$$\{\Delta \boldsymbol{R}_i\} = [\Delta R_{xi} \quad \Delta R_{yi} \quad \Delta R_{zi} \quad \Delta R_{pi}]^{\mathrm{T}},\ i=1,2,\ldots,8, \tag{4}$$

where Δu_i, Δv_i and Δw_i are the displacement increments of element node i, Δp_i is the porewater pressure increment of element node i, ΔR_{xi}, ΔR_{yi} and ΔR_{zi} are the equivalent load increments of element node i, and ΔR_{pi} is the equivalent water runoff increment of element node i.

Since groundwater seepage by excavation in soft soil not only includes negative excess porewater pressure induced by unloading, but also involves the water head difference between the inside and outside of a pit, so Eqs.(3) and (4) are not suitable for the excavation analysis. Here soil water potential is introduced. Soil water potential of saturated soil can be expressed in the following equation on condition that the solute potential of soil is neglected:

$$P=p+\gamma_{\mathrm{w}} z, \tag{5}$$

where the spatial coordinate z is upwards positive, P is the soil water potential of saturated soil, p is the sum of pressure potential and load potential, i.e. the total porewater pressure, and $\gamma_{\mathrm{w}} z$ is the gravity potential.

If the soil water potentials of element node i at $t=t_n$ and $t=t_{n+1}$ are $P_{i(n)}$ and $P_{i(n+1)}$ respectively, Eqs.(3) and (4) should transform into the following equations without regard to the influence of soil vertical displacement:

$$\{\Delta \boldsymbol{U}_i\} = [\Delta u_i \quad \Delta v_i \quad \Delta w_i \quad P_{i(n+1)}]^{\mathrm{T}},\ i=1,2,\ldots,8, \tag{6}$$

$$\{\Delta \boldsymbol{R}_i\} = [\Delta R'_{xi} \quad \Delta R'_{yi} \quad \Delta R'_{zi} \quad \Delta R'_{pi}]^{\mathrm{T}},\ i=1,2,\ldots,8, \tag{7}$$

where $\Delta R'_{xi}=\Delta R_{xi}+[\boldsymbol{K}_{cij}]P_{i(n)}$, $\Delta R'_{yi}=\Delta R_{yi}+[\boldsymbol{K}_{cij}]P_{i(n)}$, $\Delta R'_{zi}=\Delta R_{zi}+[\boldsymbol{K}_{cij}]P_{i(n)}$, and $\Delta R'_{pi}=\Delta R_{pi}-\theta \Delta t K_{sij} P_{i(n)}$.

Based on the finite element equations derived, a 3D consolidation finite element program is developed. In order to validate the program, a typical 1D consolidation question (Xie and Zhou, 2002) is analyzed as an example. The soil layer top is pervious and the bottom is impervious. Soil parameters are: Poisson's ratio μ=0.301, elasticity modulus E=3 MPa, vertical permeability coefficient $k_{\mathrm{v}}=1.0\times10^{-6}$ cm/s, and thickness of soil layer H=10 m. A load curve is shown in Fig.1 where maximum load q_0=100 kPa and time t_0=70 d.

Figs.2 and 3 show the comparisons of porewater pressure, settlement and average degree of consolidation between the FEM results and the analytical solution of 1D consolidation. The results of FEM agree

very well with those of the analytical solution, so the program can be used for effective stress analysis.

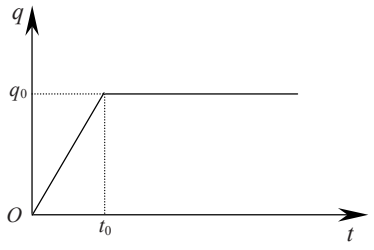

Fig.1 Loading curve

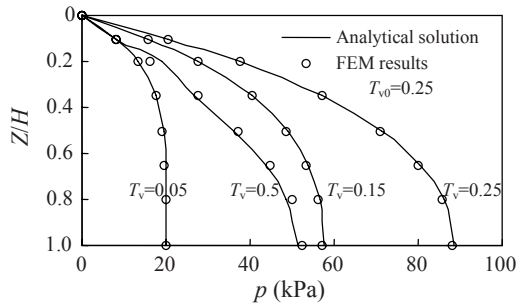

Fig.2 Comparison of porewater pressure

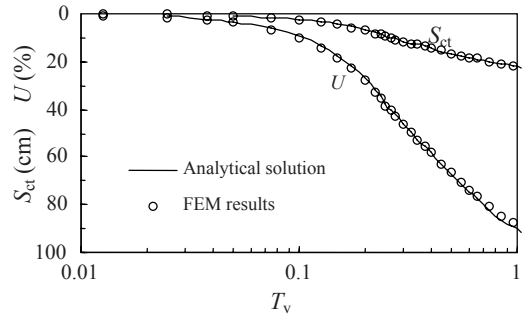

Fig.3 Comparison of settlement (S_{ct}) and average degree of consolidation (U)

INFLUENCE OF WATER HEAD DIFFERENCE ON THE EXCAVATION BEHAVIOR

Numerical example

In order to analyze the time and space effects of excavation, a numerical example is given below. The excavated length, width and depth of the foundation pit in a certain homogenous and isotropic soft soil are 60 m, 50 m and 8 m respectively. The retaining wall is 0.6 m thick and embedded 16 m deep in soft soil. Soil vertical and horizontal permeability coefficients are both 1.0×10^{-6} cm/s and effective unit weight of soil is 9.0 kN/m^3. The groundwater tables inside and outside the pit are assumed to locate on the excavated surface and the ground surface respectively.

The excavation involves three stages, and at the same time, reinforced concrete supports are accordingly set at different excavation stages and spaces between supports along the pit long side and the pit short side in every tier are 6 m and 5 m respectively. The detailed description of staged excavation of the pit is as follows:

(1) Stage 1: 2.0 m excavation depth without supports for four days, and four days' excavation intermissions for installing supports after this excavation stage.

(2) Stage 2: 3.0 m excavation depth (excavation to 5.0 m deep) with a tier of supports for six days, six days' excavation intermissions for installing next tier of supports after this excavation stage.

(3) Stage 3: 3.0 m excavation depth (full excavation to 8.0 m deep) with two tiers of supports for eight days, twenty days' excavation intermissions for casting pit base concrete after this excavation stage.

The horizontal and vertical direction boundaries are respectively located at a distance twenty-five and five times the foundation pit depth in order to minimize boundary effects. Because of the symmetry about the pit centerline only a quarter of the geometry is analyzed, so the calculating domains in x-, y- and z-direction are 100 m, 100 m and 40 m respectively. Finite element meshes of soil mass and retaining structure are shown in Fig.4. The bottom boundary is assumed to be fixed, and displacements perpendicular to the boundaries are restrained at the lateral boundaries. With regard to the hydraulic boundary conditions, a no-flow condition is assigned at the symmetrical plane and an impervious condition is assigned at the vertical boundaries; in z-direction (see Fig.4 for coordinate directions), the bottom boundary is impervious but the top is pervious; in addition, the retaining walls are double-sided impervious.

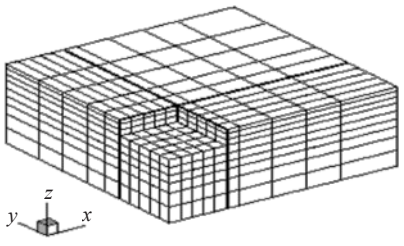

Fig.4 Mesh of finite elements

All soil units are discretized using eight-node hexahedral isoparametric elements, modelled using nonlinear Duncan-Chang model with parameters listed in Table 1, where c' and φ' are the effective cohesion and the effective internal friction angle of soil respectively, R_f is the failure ratio, and K, n, F, G, D and K_{ur} are some parameters determined by test. Retaining walls adopt Wilson non-harmony elements, modelled with linear elastic model, whose modulus of elasticity and Poisson's ratio are 25000 MPa and 0.167 respectively. A row of 0.1 m thick interfaces used to connect soil mass and retaining wall are set respectively in the two sides of the retaining wall, adopting 3D thin interface elements derived from Yin's rigid plastic model (Yin *et al*., 1995) for outer friction angle=1.0° and cohesion=0.5 kPa (Wang, 1994), and its other model parameters are the same as those of soil mass elements. Supports adopt spatial bar elements with 0.6 m×0.6 m section, with them being modelled using linear elastic model, whose elasticity modulus is 23000 MPa.

Table 1 Duncan-Chang model parameters of soil

Parameters	Values
K	150
n	0.7
R_f	0.85
c' (kPa)	15
φ' (°)	35
F	0.15
G	0.35
D	3.5
K_{ur}	300

Influence of variation of water head difference on excess porewater pressure and pit deformations

Fig.5 shows the influence of variation of water head difference on excess porewater pressure around the pit at y=0 section after the third excavation stage. When considering the variation of water head difference, negative excess porewater pressure outside the pit increases, whereas it decreases inside the pit and is positive in some area. So excess porewater pressure distribution considering the variation of water head difference is more complicated, and excess porewater pressure beneath the retaining wall has a transitional area from the negative maximal value to the positive maximal value, mainly because seepage induced by water head difference generates negative excess porewater pressure outside the pit and positive excess porewater pressure inside the pit. However, Fig.5 only shows the distribution of excess porewater pressure inside and outside the pit, not the groundwater seepage.

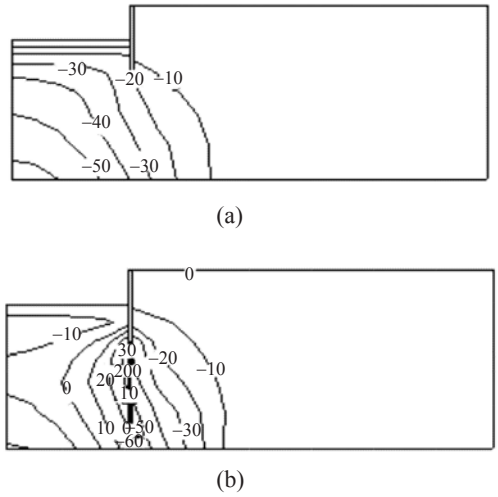

Fig.5 Distribution of excess porewater pressure inside and outside the pit (unit: kPa). (a) With no consideration of variation of water head difference; (b) With consideration of variation of water head difference

Fig.6 shows the comparison of pit deformations at y=0 section after the third excavation stage between the results considering variation of water head difference and those without considering it. The pit deformations are all larger if the variation of water head difference is considered, in which, the maximum horizontal displacement increases by 42%, the maximum ground surface settlement displacement increases by 63% and the maximum heave of pit base increases by 43%. So the result without considering the variation of water head difference is in unsafe side.

ENVIRONMENTAL EFFECTS

Time effect

To analyze the variations with time of excess porewater pressure, some test points are selected, which are illustrated in Fig.7. Fig.8 shows the variations with time of excess porewater pressures at test points. The time effect of excess porewater pressure at test point P_1 is not distinct, because this test point is near the ground surface and the excess porewater pre-

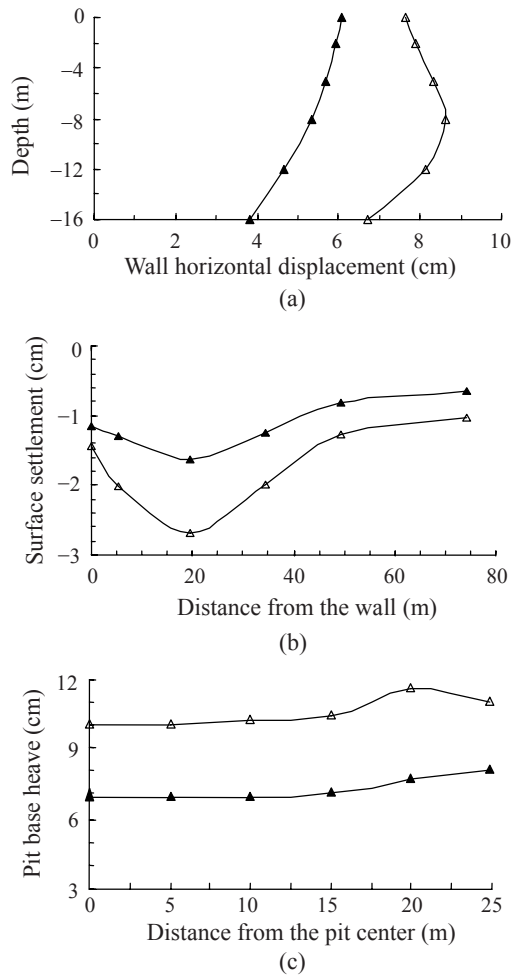

Fig.6 Comparison of the pit deformations. (a) Wall horizontal displacement; (b) Ground surface settlement; (c) Pit base heave

With no consideration of variation of water head difference

With consideration of variation of water head difference

ssure dissipates fast. The time effect of excess porewater pressure at test point P_4 is not distinct either, because this test point is far from the pit; accordingly the influence of excavation is less and excavation generates less excess porewater pressure. Since test point P_2 is near the ground surface and also far from the pit, less excess porewater pressure is generated and its time effect is not distinct either. For test points P_3, P_5 and P_6, on one hand, the influence of excavation is great, and accordingly excess porewater pressures induced by unloading and groundwater seepage are both large; on the other hand, excess porewater pressures dissipate slower since they are far from the drainage boundary, so time effects of excess porewater pressure at these test points are very remarkable.

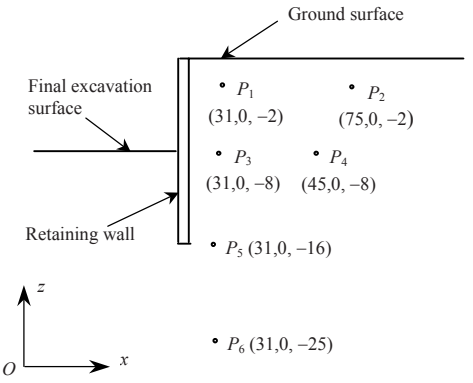

Fig.7 Sketch map of test points position

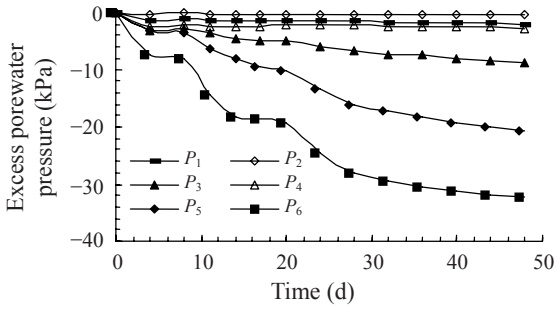

Fig.8 Variations with time of excess porewater pressures at test points

Fig.9 shows the variations with time of soil horizontal displacements at y=0 section. The soil horizontal displacements are larger near the pit (x=25.7 m) due to the greater influence of excavation. Soil horizontal displacement distributions in the depth range beneath the retaining wall base are all approximately triangular, and in the depth range above the retaining wall base, they vary from the triangular distributions during the first excavation stage without support to the middle protuberance distributions during the second and third excavation stages with support. Far from the pit (x=60 m), because of less influence of excavation, the soil horizontal displacements are less and their distributions are all approximately triangular. During excavation intermissions, the soil horizontal displacements decrease to a certain extent with excess porewater pressure dissipation, which is in accord with the investigation made by Ou and Lai (1994), especially near the retaining wall.

Fig.10 shows the variations with time of ground surface settlements behind the retaining wall at y=0 section. The maximum ground surface settlements

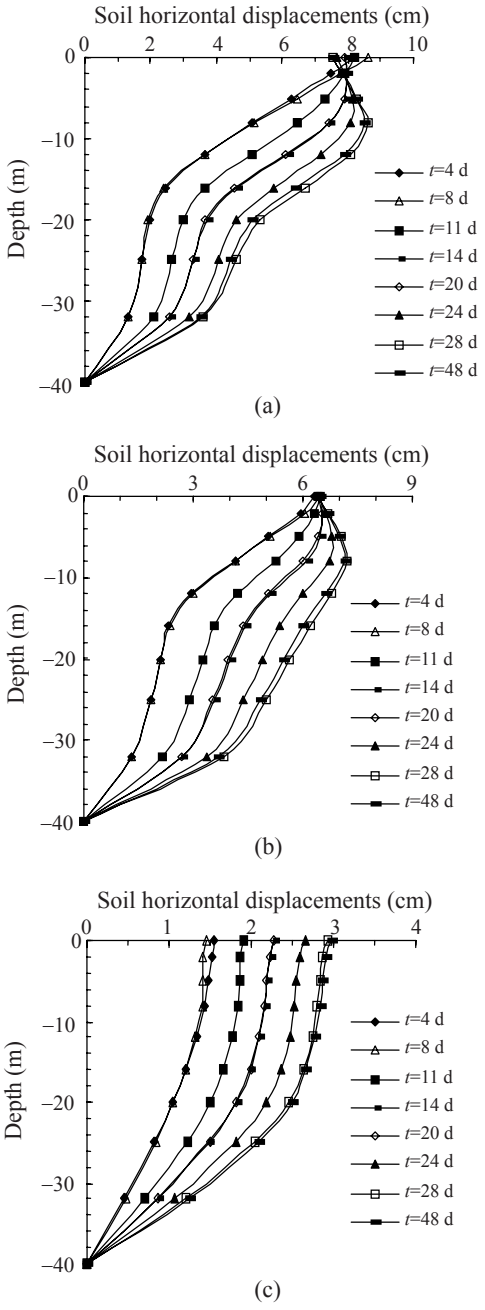

Fig.9 Variations with time of soil horizontal displacements behind the pit. (a) At x=25.7 m section; (b) At x=31 m section; (c) At x=60 m section

occur near the retaining wall during the first excavation stage without support, whereas the maximum ground surface settlements during the second and third excavation stages with support occur at about 20 m far behind the retaining wall due to the influence of support restriction and heave of soil beneath the retaining wall. So understanding the variations with time of ground surface settlement is needed so that effective measures can be taken to ensure the safety of buildings around.

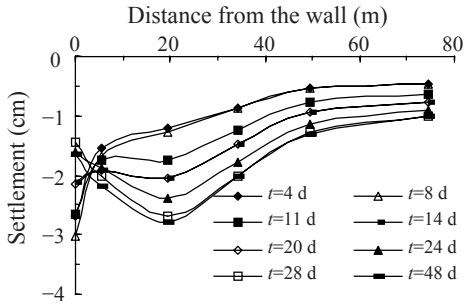

Fig.10 Variations with time of ground surface settlements

Spatial effect

Figs.5b and 11 show spatial distributions of excess porewater pressure after the third excavation stage. Compared with excess porewater pressure of the margin section (shown in Fig.11b), at the middle section (shown in Fig.5b) negative excess porewater pressure outside the pit is larger, whereas positive excess porewater pressure of the inside is less, mainly as a result of larger negative excess porewater pressure induced by unloading at the middle section.

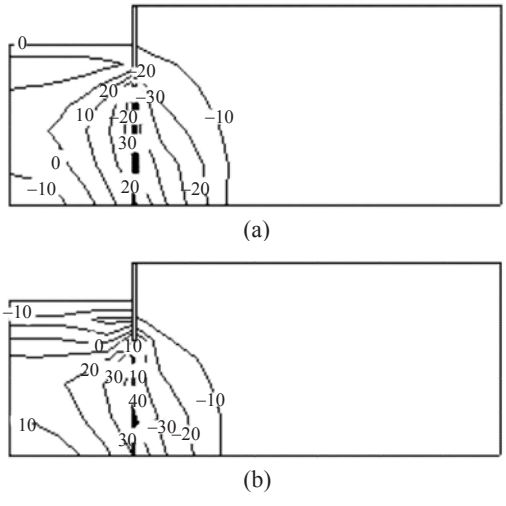

Fig.11 Spatial distribution of excess porewater pressure inside and outside the pit (unit: kPa). (a) At y=12 m section; (b) At y=24 m section

Fig.12a shows the spatial distribution of retaining wall horizontal displacements after the third excavation stage. Due to the influence of the spatial

effect of excavation, the wall horizontal displacement near the middle section is larger, whereas it is smaller near the margin section. Fig.12b shows the spatial distribution of soil horizontal displacements behind retaining walls at y=0 m section after the third excavation stage. Soil horizontal displacement is larger near a pit, and the maximum horizontal displacement occurs near the depth of excavated surface. However, soil horizontal displacement is smaller far from the pit, and the maximum horizontal displacement occurs on the ground surface.

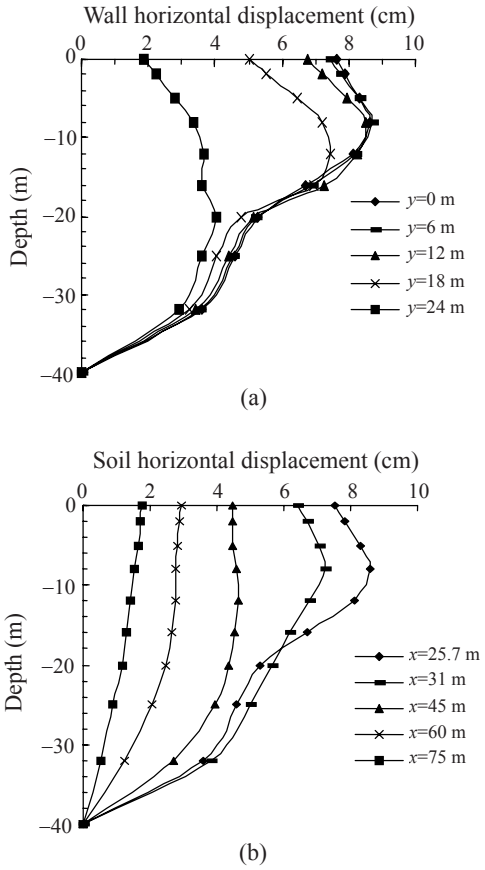

Fig.12 Spatial distributions of soil horizontal displacement behind the pit. (a) At x=25.6 m section; (b) At y=0 m section

Figs.13a and 13b show the distributions of ground surface settlement along the pit long side (i.e. y-direction) and the pit short side (i.e. x-direction) respectively. As the result of the influence of the pit spatial effect, the ground surface settlement near the middle section is larger, but is smaller near the margin section, as shown in Fig.13a. The maximum ground surface settlement occurs at about 19.4 m (x=45 m) far behind the retaining wall due to the influence of soil stratum heave beneath the retaining wall, whereas the maximum ground surface settlement at about 74.4 m (x=100 m) far behind the retaining wall is very small, and only 1.02 cm.

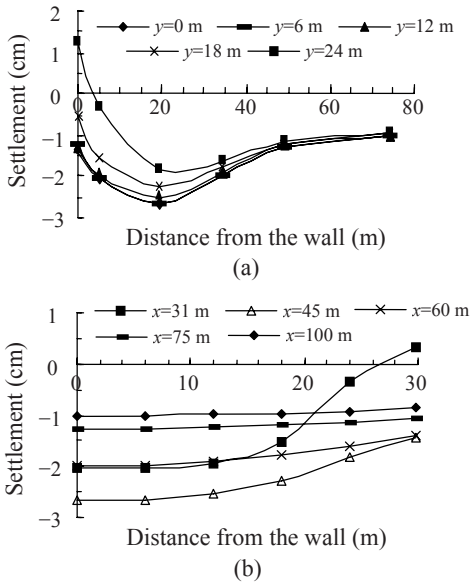

Fig.13 Spatial distributions of soil vertical displacement behind retaining wall. (a) Along y-direction; (b) Along x-direction

CONCLUSION

Based on Biot's consolidation theory, finite element equations considering the variation of water head difference between the inside and outside a pit were deduced, and the corresponding program was further developed. By investigating in detail the influence of excavation on soil movement and groundwater flow, the following conclusions can be drawn:

(1) When considering the variation of water head difference between the inside and outside of a pit, the distributions of excess porewater pressure around the pit are more complicated, and the horizontal displacement of the retaining wall, the ground surface settlement behind the retaining wall and the pit base heave are all larger. So the FEM results of excavation without considering the variation of water head difference are underestimated.

(2) Excess porewater pressures in areas near the drainage boundary and far from a pit are less and their time effects are not distinct, whereas in other areas,

they are great and time effects are very remarkable.

With the excavation time and depth increasing, the soil horizontal and vertical displacements both gradually get large. The distribution shapes of soil horizontal displacements far from the pit are approximately triangular on the whole, but those near a pit are irregular. The maximum ground surface settlement occurs near the retaining wall at the first excavation stage without support, but occurs in a certain area behind the retaining wall at the second and third excavation stages with supports. The soil horizontal displacements decrease to a certain extent with excess porewater pressure dissipation during excavation intermissions.

(3) The maximum horizontal and vertical displacements of soil behind the retaining wall near the middle section are both larger than those near the margin section due to the spatial effect of excavation.

References

Duan, S.W., Shen, P.S., 2005. Analysis of nearby pipeline damage induced by deep excavation. *Engineering Mechanics*, **22**(4):79-83 (in Chinese).

Hou, X.Y., Chen, Y.F., 1989. Evaluation of settlement in surrounding soil medium produced by deep exvavation. *Geotechnical Engineer*, **1**(1):3-13 (in Chinese).

Ou, C.Y., Lai, C.H., 1994. Finite element analysis of deep excavation in layered sandy and clayey soil deposits. *Canadian Geotechnical Journal*, **31**:204-214.

Ping, Y., Bai, S.H., Xu, Y.P., 2001. Numerical simulation of seepage and stress coupling analysis in deep foundation pit. *Rock and Soil Mechanics*, **22**(1):37-41 (in Chinese).

Shi, C.H., Peng, L.M., 2006. Ground surface settlement caused by foundation pit excavation and dewatering. *China Civil Engineering Journal*, **39**(5):117-121 (in Chinese).

Wang, G.G., 1994. Theoretical Study on Large Strain of Deep Excavation. Ph.D Thesis, Tongji University, Shanghai (in Chinese).

Whittle, A.J., Hashash, Y.M.A., Whitman, R.V., 1993. Analysis of deep excavation in Boston. *Journal of Geotechnical Engineering, ASCE*, **119**(1):69-90. [doi:10.1061/(ASCE)0733-9410(1993)119:1(69)]

Xie, K.H., Zhou, J., 2002. Theory and Application of Finite Element Analysis in Geotechnical Engineering. Science Press, Beijing (in Chinese).

Xie, K.H., Liu, C.M., Ying, H.W., Yang, W., 2002. Analysis of settlement induced by dewatering during excavation in layered soil. *Journal of Zhejiang University (Engineering Science)*, **36**(3):239-242 (in Chinese).

Yin, Z.Z., Zhu, H., Xu, G.H., 1995. A study of deformation in the interface between soil and concrete. *Computers and Geotechnics*, **17**(1):75-92. [doi:10.1016/0266-352X(95)91303-L]

Zdravkovic, L., Potts, D.M., St John, H.D., 2005. Modelling of a 3D excavation in finite element analysis. *Geotechnique*, **55**(7):497-513.

Zhang, M.J., Song, E.X., Chen, Z.Y., 1999. Ground movement analysis of soil nailing construction by three-dimensional (3-D) finite element modeling (FEM). *Computers and Geotechnics*, **25**(4):191-204. [doi:10.1016/S0266-352X(99)00025-7]